Pacific Northwest NATIONAL LABORATORY

PNNL-30066

Preliminary Design Process for Networked Microgrids

June 2020

Kevin P Schneider[1]
Harsha Nagarajan[2]
Annabelle Pratt[3]
Mathew J Reno[4]
Ben Ollis[5]
Francis Tuffner[1]
Sai P Nandanoori[1]
Soumya Kundu[1]
Wei Du[1]
Hassan Hijazi[2]
Rishabh Jain[3]
Francisco Flores-Espino[3]
Joshua Hambrick[5]
Dan Ton[6]

U.S. DEPARTMENT OF ENERGY

Prepared for the U.S. Department of Energy
under Contract DE-AC05-76RL01830

1 Pacific Northwest National Laboratory
2 Los Alamos National Laboratory
3 National Renewable Energy Laboratory
4 Sandia National Laboratories
5 Oak Ridge National Laboratory
6 U. S. Department of Energy

PACIFIC NORTHWEST NATIONAL LABORATORY
operated by
BATTELLE
for the
UNITED STATES DEPARTMENT OF ENERGY
under Contract DE-AC05-76RL01830

Printed in the United States of America

Available to DOE and DOE contractors from
the Office of Scientific and Technical Information,
P.O. Box 62, Oak Ridge, TN 37831-0062
www.osti.gov
ph: (865) 576-8401
fox: (865) 576-5728
email: reports@osti.gov

Available to the public from the National Technical Information Service
5301 Shawnee Rd., Alexandria, VA 22312
ph: (800) 553-NTIS (6847)
or (703) 605-6000
email: info@ntis.gov
Online ordering: http://www.ntis.gov

PNNL-30066

Preliminary Design Process for Networked Microgrids

June 2020

Kevin P Schneider
Harsha Nagarajan[1]
Annabelle Pratt[2]
Mathew J Reno[3]
Ben Ollis[4]
Francis Tuffner
Sai P Nandanoori
Soumya Kundu
Wei Du
Hassan Hijazi[1]
Rishabh Jain[2]
Francisco Flores-Espino[2]
Joshua Hambrick[3]
Dan Ton[5]

Prepared for
the U.S. Department of Energy
under Contract DE-AC05-76RL01830

Pacific Northwest National Laboratory
Richland, Washington 99354

1 Los Alamos National Laboratory
2 National Renewable Energy Laboratory
3 Sandia National Laboratories
4 Oak Ridge National Laboratory
5 U. S. Department of Energy

Abstract

Changes in economic, technology, and environmental policies are resulting in a re-evaluation of the dependence on large central generation facilities and their associated transmission networks. Emerging concepts of smart communities/cities are examining the potential to leverage cleaner sources of generation, and the potential to integrate electricity generation with other municipal functions. When grid-connected, these generation assets can supplement the existing interconnections with the bulk transmission system, and in the event of an extreme event, they can provide power via networks of microgrids. While the design process for a single stand-alone microgrid is relatively well understood, the process of designing the infrastructure for networked microgrid operations has not been well studied. Because of the wide range of potential operational goals for microgrids, it is typical to follow the engineering process of developing an initial conceptual design, a preliminary design, a detailed design, and then a final as-built design. The conceptual design is typically completed without detailed engineering analysis, and the preliminary design is the first stage that requires it. This paper presents a process for developing the preliminary design for networked microgrids, which can then be used as a basis for the final as-built design.

Summary

This report is prepared as part of a multi-laboratory effort funded by the United States (US) Department of Energy (DOE) Advanced Grid Research Program. This report covers the networked microgrid program efforts which were led by the Pacific Northwest National Laboratory (PNNL) in fiscal year (FY) 18 and 19 as part of the DOE microgrid program managed by Mr. Dan Ton.

This report focuses on the initial development of the open-source optimal design and operations (OD&O) tool. The OD&O tool was being developed by the Los Alamos National Laboratory (LANL), supported by PNNL, the National Renewable Energy Laboratory (NREL), Sandia National Laboratories (SNL), and Oak Ridge National Laboratory (ORNL). This report outlines the development work on the OD&O tool including the first early version release.

Acknowledgments

Contributions to this project were achieved through United States (US) Department of Energy (DOE) Advanced Grid Research Program. The views expressed in the article do not necessarily represent the views of the DOE or the United States Government.

The Pacific Northwest National Laboratory is operated by Battelle for DOE under Contract DE-AC05-76RL01830.

This work was authored in part by the National Renewable Energy Laboratory, operated by Alliance for Sustainable Energy, LLC, for DOE under Contract No. DE-AC36-08GO28308.

Sandia National Laboratories is a multi-mission laboratory managed and operated by National Technology & Engineering Solutions of Sandia, LLC, a wholly owned subsidiary of Honeywell International Inc., for DOE's National Nuclear Security Administration under contract DE-NA0003525.

Contents

Figures

1.0 Introduction

Modern electric power systems face the dual challenges of an increasing number of operational threats and increased expectations for service, provided at the lowest possible cost [1]-[3]. However, building electrical infrastructure that is resilient to all possible hazards, for all end-use loads, is not always cost-effective [4]. As an alternative to upgrading the entire system, islanded microgrids have proven to be effective at supporting critical loads during extreme events [5]-[8]. An individual microgrid has several advantages over traditional dedicated backup generation. Similar to the economies of scale that were realized when the early Edison Power Systems were interconnected in the 19th century, microgrids realize benefits by coordinating the operation of distributed energy resources (DERs). The realized benefits include a reduction in the number of required generators, increased operational efficiencies, and increased system reliability [9]. Despite their high initial capital cost, operational microgrids have proven their ability to achieve these benefits around the world. An extension of the individual microgrid is the concept of networked microgrids. A networked microgrid is the electrical interconnection of two or more individual microgrids that may or may not be connected via communications and/or control [10]. Networking can be accomplished by electrical interconnection at primary or secondary distribution voltages, and even at sub-transmission voltages. The networking of microgrids allows for further economies of scale, while maintaining independence from generating units that may be geographically separate [10]. Networked microgrids allow for local economies of scale to be leveraged for efficiency, and for improvements in system reliability and resiliency. According to a United States (US) Department of Energy (DOE) report [10], networked microgrids have the technical potential to reduce the utility cost of serving the microgrids by at least 10%. In addition, during extreme event outages they have the potential to improve customer-level reliability and resilience by:

- extending the duration of electrical service to critical loads by at least 25%;
- maintaining electrical service for all critical loads during a single generator contingency in any microgrid; and
- lowering capital expense by at least 15%.

While networked microgrids have the potential to provide additional operational benefits, they are significantly more complex in regard to operation and control than individual microgrids [11]. The complexity of networked microgrid operations can be attributed to a combination of controls [12] and the dynamics of operations [13], [14]. The operational complexities can be seen in the simplest examples of networked operations, when they are nested [15] or directly adjacent to one another [16]. Even in these simple examples of networking, each deployment has required extensive one-off simulation and analysis to support; the existing analysis tools are not able to examine the full range of networked microgrid operations. As a result, it is difficult for the design process to progress from the initial conceptual design to a final detailed design. Developing a final design process for networked microgrids is complicated because the of large number of operational scenarios made possible by variations in individual microgrids, their internal controls, and variation in generation sources. However, if a preliminary design can be completed, then the number of operational scenarios that must be evaluated for the detailed design can be reduced. To complete a preliminary design, a set of operational requirements that must be met for all networked microgrids is considered. These include the abilities to supply the end-use loads at an acceptable cost, to maintain stability, and to protect the system from the anticipated range of power system faults [10]. This paper presents a design process (methodology) that enables the development of a preliminary design for networked microgrids operations given a set of operational constraints; specifically, determining the cost-optimal solution for networking pre-existing individual microgrids for resiliency applications. An example of the design process is presented using an open-source optimal design and operations (OD&O) tool developed for the US DOE [17].

2.0 Networked Microgrid Overview

The economic performance and viability of microgrids depend on the technical capabilities of the microgrid, the local regulatory context, and the business model that the microgrid owners choose to monetize the services provided by their system [18]. The work described in this paper focused primarily on designing the technical capabilities, and regulatory and business concerns were considered part of the optimization to determine revenue generation potential. For any AC electric power system, it is necessary to have the generating units, controls, and capabilities to maintain a stable frequency and voltage, and to supply the end-use loads [19], [20]. In addition, for a microgrid, the system must remain dynamically stable in the absence of a stiff voltage source and must be protected from the expected range of power system faults. Figure 1 shows an idealized image of how microgrids could be networked.

Figure 1. An idealized network of microgrids.

The microgrids shown in Figure 1 represent a selection of the microgrid types defined in IEEE std. 1547-2011 [21]. The four microgrids shown in Figure 1 would be defined in IEEE std. 1547-2011 as (1) Facility Island (single residential meter), (2) Secondary Island (multiple residential meters), (3) Secondary Island (multiple industrial meters), and (4) Lateral Island. The differences in the microgrids shown in Figure 1 highlight some of the operational challenges of developing a design for networked microgrid operations. Specifically, the variability in size, generation compositions, and physical separation represent a large number of variables that are interdependent, resulting in a large number of possible decisions.

3.0 Design methodology

Because of the complexities of networking individual microgrids there is no generalized approach to their design. These complexities include, but are not limited to, potential interactions between individual microgrid controllers, an increased number and mix of DERs compared to individual microgrids, and the switching requirements for interconnection, all of which make the design of networked microgrids difficult. However, the design process commonly used for individual microgrids can be extrapolated for networked microgrids. This process typically includes a series of design stages that narrows down options until finally arriving at the final as-built system [7], [15], [17], as shown in Figure 2 and defined below.

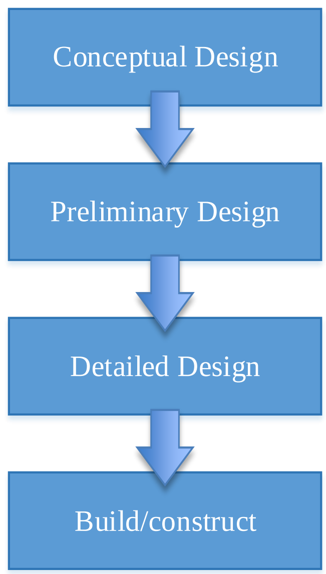

Figure 2. Idealized engineering design process.

- Conceptual: Issues such as type and size of generation, level of load participation, and classes of control schemes to be included are evaluated during the conceptual design stage.
- Preliminary: In the preliminary design stage, the next level of detail is added such as the ratings of the generating units and whether lines should be upgraded or constructed. The preliminary design stage is when the proposed approach, demonstrated with the OD&O tool in this paper, can be used.
- Detailed: The detailed design collapses the “possible” options of the preliminary design into a single option that addresses the specific operational requirements. This includes specific manufacturers of generating units and the specific controls that will be used.
- Build/construct: During this stage, the system is built, commissioned, and its performance is verified. The output is the final design and it contains the formal records of the system as built.

Thousands of microgrids have been deployed around the world using variations of this process, and there is a high degree of variability. There is no standard procedure for the analysis of microgrids, or networked microgrids, and this contributes to the high cost of their deployment.

This section presents a design methodology/approach for developing a preliminary design for networking pre-existing individual microgrids for resilient applications, based on determining the cost-optimal solution. At a minimum, an operational microgrid must have the ability to cost-effectively supply the end-use loads within acceptable voltage ranges, be dynamically stable, and provide coordinated protection against power system faults. The following sections describe how to develop a preliminary design based on the optimization at cost, subject to the constraints of the system remaining dynamically stable and being able to implement protection coordination. The OD&O tool [17] is used as an example implementation of the proposed process.

3.1 Optimization of Capacity at Economy

The first basic requirement is to cost-effectively supply the end-use loads within the acceptable voltage ranges without overloading any equipment. This can be formulated as an optimization problem of minimizing the net investment cost of the new components (such as lines, conventional generators, storage devices, switches, and re-closers) and the hardening of existing components in independent microgrids over a finite time horizon. For simulation purposes, this paper uses the finite time horizon of one-year at one-hour time intervals, which leads to 8640 time periods. To address the computational complexity of an annual time horizon, a typical-day approach, as discussed in the next sections, will be used [17]. This approach aggregates similar day load profiles, thus reducing the total number of representative days to 14, resulting in only 336 time periods. Finally, this cannot be an unconstrained optimization, or else it could lead to non-feasible results.

To address the electrical characteristics of the physical infrastructure, the optimization is constrained by electrical limits. The engineering-based constraints should include (1) three-phase unbalanced power flow using Distflow; (2) engineering limits (e.g., line thermal ratings, voltage ratings, and generator operating limits); (3) storage device charging-discharging efficiency curves; and (4) time-coupling constraints including the ramping of generators and state-of-charge for the storage devices.

The overall algorithm is outlined in detail in Figure 3. The two primary parts of the algorithm are the “Outer-Layer optimization” and the “Resilience-Layer optimization.” As part of the OD&O tool of [17], at each layer, a mixed-integer nonlinear program (MINLP), using state-of-the-art solvers such as Ipopt/Juniper [22], is used.

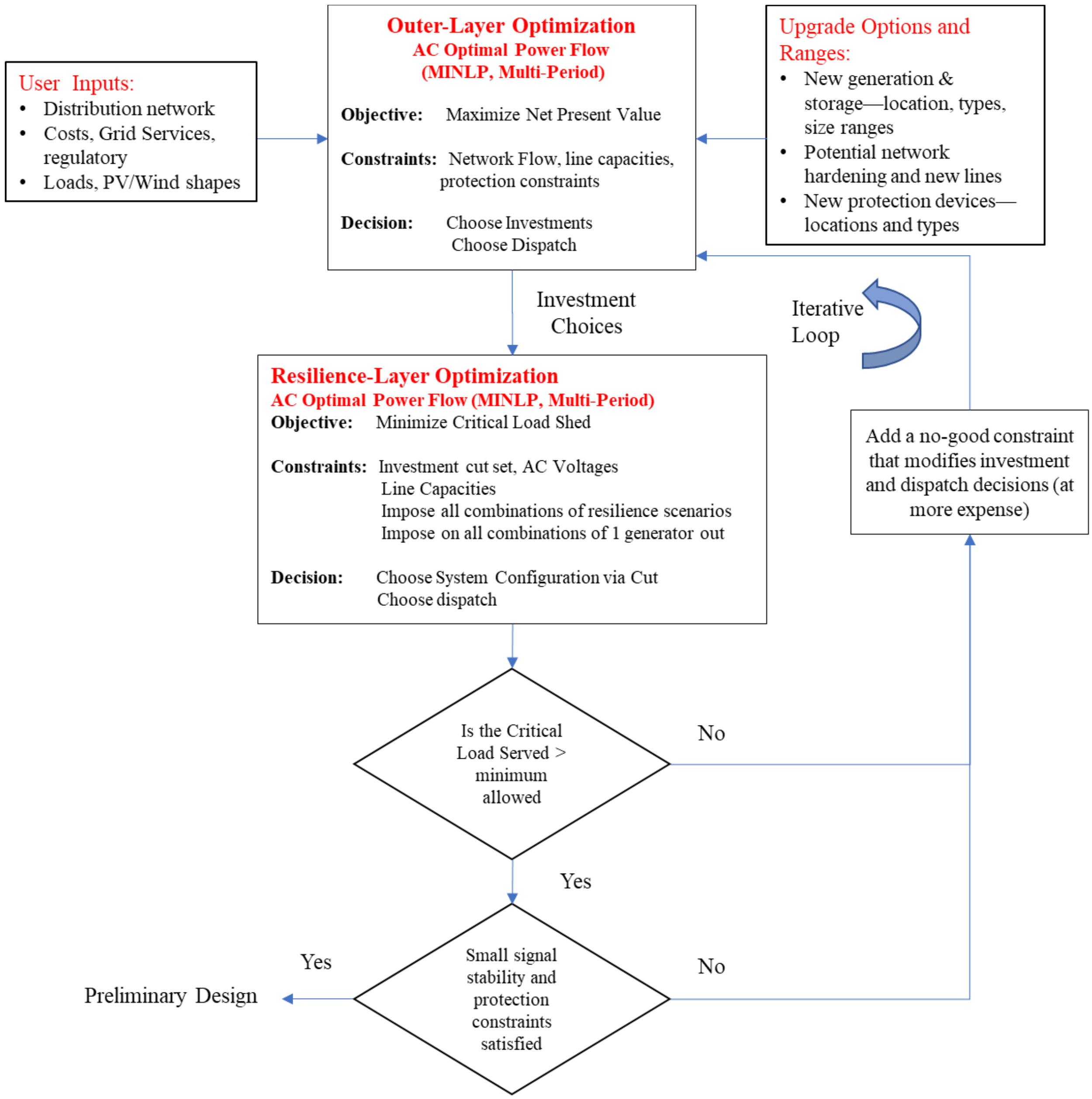

Figure 3. Algorithm outline for the development of networked microgrid preliminary design.

3.1.1 Outer-Layer Optimization

In the Outer-Layer of the algorithm, the process solves a multi-period mixed-integer nonlinear optimization problem. The user inputs for this layer include the network model of existing microgrids, associated costs of component upgrades (such as additional generation resources, additional power lines, switch gear, and battery storage devices), along with the load and PV/wind profiles, and costs of grid and regulatory services.

The objective function of the Outer-Layer optimization maximizes the net present value of the combined microgrids, which includes the minimization of investment costs and maximization of operations revenue. It is in the Outer-Layer that the specific investment options can be defined. For example, will the options include new lines, line hardening, and/or battery deployments? Numerous options can be included, but at a cost of computational complexity due to the increased size of the search space. The constraints of the Outer-Layer problem are three-phase unbalanced power flow and engineering limits (e.g., line thermal capacities and node-voltages). Currently, microgrid stability and protection constraints are not in the Outer-Layer optimization, and instead are imposed as post-optimization constraints, as described in the next section. This section focuses on the power-flow-based constraints.

Because the majority of distribution systems are operated radially, a radial operating condition is assumed for the unbalanced three-phase power flow, with the nonlinear, nonconvex Distflow equations are given by (1).

$$S_{ij}^{\phi I} = V_i^{\phi I} \sum_{J \in \varphi_{ij}} \left(Y_{ij}{}^{\phi_I \phi_J}\right)^* \left(V_i^{\phi_J} - V_j^{\phi_J}\right)^* \forall I \in \varphi_{ij}, ij \in E \tag{1}$$

where,

$|S_{ij}^{\phi_I}| \leq T_{ij}^{\phi_I} \; \forall I \in \varphi_{ij}, ij \in E$

where, E represents the set of all three-phase lines in the network, φ_{ij} represents the set of phases on every line ij, $Y_{ij}^{\phi_I \phi_J}$ represents the complex admittance value corresponding to phases ϕ_I and ϕ_J of line $ij \in E$, $V_i^{\phi_I}$ represents the complex voltage on phase ϕ_I on bus i, $S_{ij}^{\phi_I}$ and $T_{ij}^{\phi_I}$ represent the complex apparent power flow and thermal limit of phase ϕ_I of line $ij \in E$, respectively, $(\cdot)^*$ and $|\cdot|$ represent the conjugate and magnitude of a complex number, respectively. For ease of viewing, the subscripts of time 't' are removed because these equations hold true for every time period within the given horizon. For the optimization, the phase components (superscripts $\phi_I, I \in \varphi_{ij}$) on every line can be transformed into sequence components consistent with the power engineering literature.

The above Distflow equations are computationally challenging because of the inherent non-convexity of the solution space. However, solvers such as Ipopt/Juniper can ensure feasibility for the set of equations in (1) without guaranteeing global optimality. Given the above constraints, and applying Kirchhoff's current law at every electrical node, the Outer-Layer optimization problem can be modeled as an MINLP using discrete variables to represent the on/off status of different investment options.

For brevity purposes, the time-coupled unit commitment constraints modeled with generator on/off status are not included in this paper. The extended formulation of the detailed time-coupled formulation is presented in [23], [24]. The outputs of the Outer-Layer optimization are the investment decisions and the dispatch values of the generators and battery storage devices.

Considering the complexity of the MINLP to be solved in the outer layer, the following simplification strategies are implemented to make the problem tractable:

(1) *The typical-day approach*: The main goal of this simplification is to reduce the number of time steps used to represent the load profiles by aggregating similar day profiles into a single day. This approach has proved to be very effective in the literature [23], [25] and hence is used in this methodology. Figure 4 shows the graphical description of the typical-day approach on a simplified load profile at a single node. This works particularly well for aggregating typical weekday and weekend profiles.

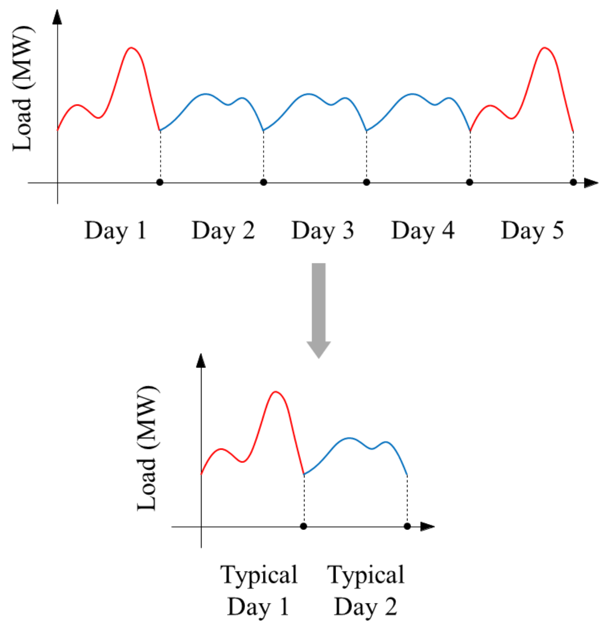

Figure 4. Example of the typical-day approach.

(2) *Convex relaxations for non-simultaneous charging and discharging states of battery storage devices*: This relaxation approach is applied to circumvent the representation of battery efficiency curves using auxiliary discrete variables, which increases the combinatorial complexity of the problem. This approach, which is effective on simpler versions of the microgrid planning and operation problem [24], [26], is applied in the Outer-Layer optimization

3.1.2 Resilience-Layer Optimization

Given the investment-decision options from the Outer-Layer optimization, the Resilience-Layer ensures that the investment decisions made by the Outer-Layer results in a resilient system for the duration of extreme events such as hurricanes, earthquakes, or other events. To this end, the outer loop decisions are accepted only if the total amount of critical loads (e.g., wastewater treatment and emergency shelters) served during an extreme event satisfies a user-defined bound.

As shown in Figure 3, the objective of this optimization problem is to minimize the total critical load shed subject to the three-phase unbalanced power flow and other constraints. In addition, this optimization is performed over a range of damage scenarios, discretely sampled from the probabilistic damage models, as discussed in [23].

The Resilience-Layer Optimization is only applied for the duration of an extreme event with the corresponding sampled discrete damage scenarios. To this end, the problem is solved using a scenario-based decomposition approach, typically applied for two-stage optimization problems, to keep the problem tractable at every time step [27]. If the minimum critical load shed from this step is greater than the minimum allowed value, then a “no-good cut” is added to the current investment decisions as described in the next section.

3.1.3 No-Good Cuts for Resiliency Loops

Because the two optimization layers are independent with respect to optimization, it is possible for some preliminary solutions from the Outer-Layer optimization to violate conditions of the Resilience-Layer. To address this issue an iterative approach is taken. Let x^* represent the binary vector of investment choices obtained as the solution from the Outer-Layer optimization. If x^* violates the Resilience-Layer optimization problems, the following valid inequality is added back to the Outer-Layer problem to be resolved:

$$\sum_{i \in S(x^*)} x_i \leq (|i \in S(x^*)| - 1) \tag{2}$$

where:
$S(x^*) := \{i: x_i^* = 1\}$

Iteratively solving the Outer-Layer problem with the above-mentioned cuts is guaranteed to converge to an optimal design and operational solution, which satisfies the metrics of resilience. This algorithm has a *finite convergence* given that there are only a finite number of feasible discrete solutions to the Outer-Layer problem. The power flow constraints are included within the core optimization, but it is also necessary to ensure dynamic stability and protection of the solution from the reliability perspective of operating networked microgrids. In the current version of the OD&O tool the stability and protection constraints are verified after the optimization process. However, work is ongoing to include these constraints in the core optimization so that they are treated as constraints within the optimization. The following section explains how the constraints are being formulated as part of the ongoing work to include them in the core optimization loops.

3.2 Stability Constraints

In [28], power system stability is described as the ability of the system to regain a state of operating equilibrium after a physical disturbance. In the IEEE/International Council on Large Electric Systems (CIGRE) joint task force paper of [28], bulk power system stability was broadly classified into (1) rotor angle stability, (2) frequency stability, and (3) voltage stability [29], [30], based on their different timescales and modes of instability. Based on the type and size of disturbances, the different forms of stability can be further classified into small-disturbance and large-disturbance, and short-term and long-term stability.

The work of [20] extended these definitions to microgrids, which is necessary because of the significantly shorter time frames for stability. For example, in a large interconnected power system it was noted in [28] that the timescales for rotor angle stability are typically less than 20 seconds and the timescales for frequency stability are between a few seconds and a couple of minutes, while voltage stability phenomena can stretch for up to tens of minutes. For microgrids the timescales are much shorter [8], [9], [13].

3.2.1 Stability in Microgrids

Unlike the large synchronous generators in the bulk transmission system, the majority of generation sources in microgrids are small distributed units often interfaced with droop-controlled inverters. In a review of stability issues in microgrids [31], it was noted that stability depends on the type of the microgrid (utility, facility, or remote), mode of operation (islanded or grid-connected), network parameters, and the control topology of the power electronic converters. In particular, the small-signal stability of microgrids has received significant attention in the literature, because ensuring small-signal stability is a necessary prerequisite before other forms of stability can be examined.

Grid-forming inverters using voltage source converters and droop-control loops are being increasingly adopted because of their ability to regulate voltage and frequency in the autonomous operation of islanded microgrids [32]. The droop gains associated with the inverters outer power control loops, as well as the network configuration, have become recognized as being defining factors for the dominant low-frequency eigen-modes, which determine the small-signal stability [33], [34]. In addition, loading conditions as well as network parameters have also been shown to affect the stability conditions [36].

For the preliminary design, small-signal stability is considered a requirement for any level of operation, and thus it is examined. Voltage and other types of frequency stability would be examined at the detailed design level when specific controllers are selected.

3.2.2 Small-Signal Stability Constraints

In the context of designing a stable networked microgrid, a necessary first step is to identify the range of values of the design parameters that guarantee the small-signal stability of the network around the desired operating point(s). The small-signal stability of a microgrid is strongly dependent on the network parameters (line impedance, loading) and inverter outer control loops (droop gains) [33], [34].

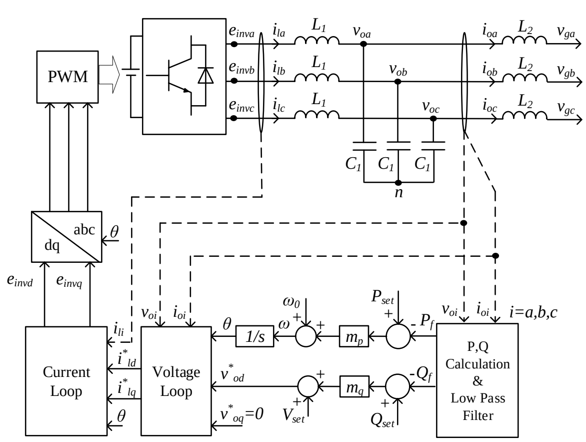

Figure 5. The controller block diagram of a multi-loop droop-controlled inverter.

Grid-forming inverters are designed to behave as a voltage source regulating both the voltage magnitude and frequency at (or near) its terminal. The inverters have a nested control architecture, as shown in Figure 5. The outer control loops determine the power-frequency and volt-VAR set points based on the droop slopes, m_p and m_q, and the active and reactive power set points, P_{set} and Q_{set}. The inner control loops include the voltage and current control loop, which ensure that the outer loop control set points are closely tracked.

When modeling the network dynamics using dynamic phasor analysis and ignoring the higher speed inner control loops, the small-signal model of the microgrid can be described compactly in the form of a parametric linear time-invariant system [37], [38]:

$$\dot{x} = A(\lambda)x \tag{3}$$

where x is the state vector that contains the phase angle, frequency, and voltage magnitude at the inverter terminals; $A(\lambda)$ is the system matrix as a function of λ, which is the parameter vector that may contain the parameters of interest, i.e., droop gains, X/R ratios of lines, conductor size, etc. The microgrid is small-signal stable if and only if the eigenvalues of the system matrix lie on the left-half plane [19]. Identifying the parametric stability region using eigenvalue analysis, however, is computationally inefficient; the complexity grows exponentially with the number of parameters. A closed-form inner approximation of the stability region is often computationally more tractable and desirable, because (1) closed-form expressions can be easily incorporated as a constraint, and (2) inner approximation of the stability region naturally safeguards against modeling inaccuracies. Lyapunov functions analysis provides a tractable and certified, albeit conservative, closed-form estimate of the parametric stability region. In particular, applying LaSalle's principle [39], the small-signal stability of the microgrid can be guaranteed by the existence of a positive definite matrix $\Psi(\lambda)$ and a negative semi-definite matrix $\Pi(\lambda)$ that satisfy the following conditions:

$$\Pi(\lambda) = \Psi(\lambda)A(\lambda) + A(\lambda)^T\Psi(\lambda) \tag{4}$$

Moreover, using transformation matrices T_1 (full-rank) and T_2, one can define block-diagonal matrices $\widetilde{\Psi}(\lambda)$ (positive definite) and $\widetilde{\Pi}(\lambda)$ (negative semi-definite) such that:

$$\Psi(\lambda) = T_1^T\widetilde{\Psi}(\lambda)T_1 \tag{5}$$

$$\Pi(\lambda) \geq T_2^T\widetilde{\Pi}(\lambda)T_2 \tag{6}$$

As was shown in [36], with an appropriate choice of the transformation matrices the block-diagonal matrices Π and Ψ have the same structure as the network configuration, thereby leading to closed-form distributed stability conditions involving the droop gains and line parameters related to each pair of neighboring inverters [49].

3.2.3 Small-Signal Stability Constraints

As an illustrative example, a small two-inverter microgrid is shown in Figure 6 with constant impedance loads.

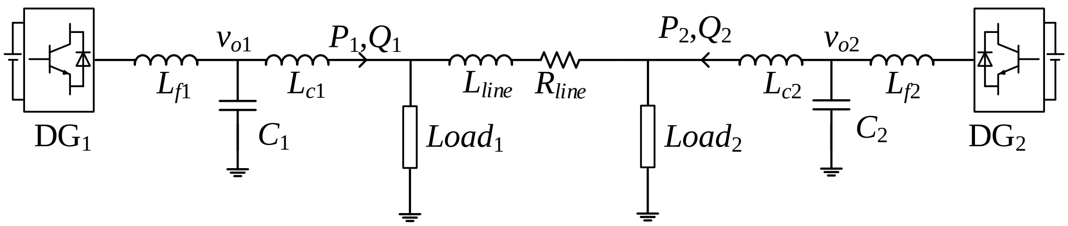

Figure 6. A small microgrid network with two droop-controlled inverters and constant impedance loads.

Various parameters such as active power-frequency (*P-f*) and reactive power-voltage (*Q-V*) droop gains, m_p and m_q respectively in Figure 5; line conductor thickness; and load values have an impact on the small-signal stability of the system. Stability margins computed using eigenvalues analysis are compared with the analytical closed-form expressions, as shown in Figure 7. In Figure 7, the results are shown comparing the stable droop gains with and without the presence of load, where the presence of load results in a smaller stability region. Droop gains for both active power and reactive power are considered, corresponding to m_p and m_q in Figure 5.

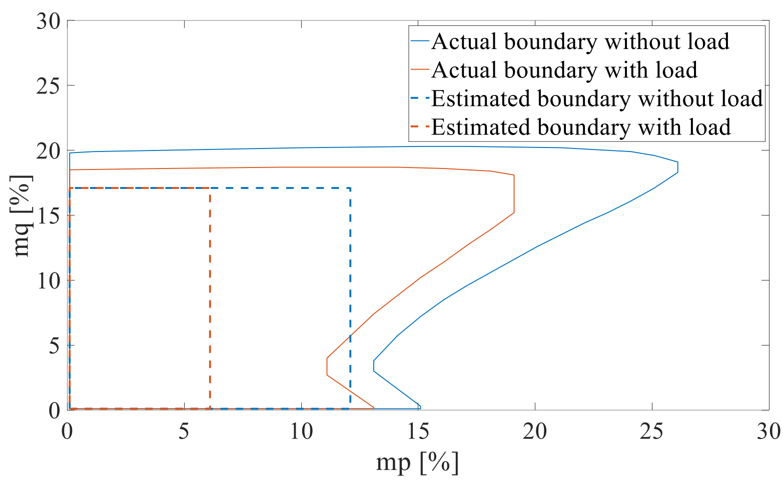

Figure 7. Comparison of stability margins (allowable droop gains) calculated using eigenvalue analysis ("actual boundary") and closed-form expressions (“estimated boundary”).

Another example in Figure 8 shows how the conductor size (cross sectional area) affects the stability margin; thicker conductors result in a smaller range of allowable *P-f* droop gains, m_p, as shown in Figure 5. Note that while the stability analysis framework is applicable to general microgrid networks, the particular findings presented in Figures 7 and 8 are only specific to the example in Figure 6 and may not be generalizable

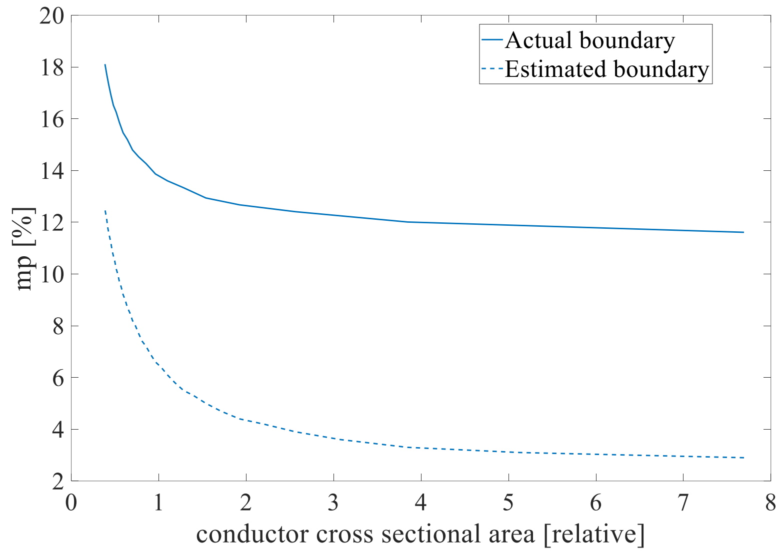

Figure 8. Effect of varying conductor cross sectional area on stability margin (allowable P-f droop gain, mp) using eigenvalue analysis ("Actual boundary") and closed-form expressions ("estimated boundary").

From Figures 7 and 8, it can be seen that the eigenvalue analysis always generates a stable region, even if it is overly conservative. Given that the presented methodology is part of a preliminary design, a conservative answer is acceptable because the goal is to verify design feasibility, not to develop a final design. While, the approach described in the previous sections for ensuring stability is integrated as a post-optimization verification, as shown in Figure 5, future work will examine integrating it into the optimization loops

3.3 Protection Constraints

The objective of protection is to detect and remove faulted sections of the network, while minimizing the amount of the network that is disconnected [40]. Protection is important to prevent damage to equipment, minimize hazards to people, maintain high service reliability, and preserve the stability of un-faulted sections of the system.

3.3.1 Microgrid Protection

Microgrids present unique challenges for protection because of their associated shorter electrical distances that make coordination challenging, their ability to dramatically change configuration (e.g., grid-interconnected mode vs. grid-isolated or islanded mode), and their inclusion of DERs that can affect the system significantly with their intermittent output. Microgrids often have low system inertia and sensitive loads that may require faster protection operation to rapidly detect and isolate faults to ensure stable recovery [41]. Microgrids that have a large percentage of inverter-based generation also present a challenge because of their relatively low fault currents.

Many protection schemes have been developed for microgrids [42], [43] and their cost and implementation details vary widely for the different microgrids. In each case, the protection scheme is developed using conventional protection techniques applied to the given topology and sources of the individual microgrid. Some authors have investigated optimization algorithms to determine the placement and settings of protection devices [44], but these algorithms focus on fixed topologies and distribution systems that have a single fault current path, and they do not account for critical loads or backup generators.

3.3.2 Protection Constraints

Networked microgrid designs must be protectable if industry is to adopt them. To accomplish this, a wide variety of protection technologies and philosophies may be used, including traditional methods such as overcurrent elements/fuses or communication-based approaches such as transfer trip protection. Protection can be a significant portion of a microgrid's cost, so optimization with cost as an objective should consider protection. Because the method presented here is used to produce a preliminary design, it is not necessary to produce a fully designed protection system. Instead, the goal is to design a networked microgrid system that can be protected using common methods.

The first step in this approach is to develop optimization constraints for the following various protection functions (ANSI protection numbers in parentheses): instantaneous overcurrent (50), timed overcurrent (51), differential protection (87), undervoltage (27), overvoltage (59), etc. [40]. In Figure 9, a simple example using a radial circuit with no downstream DER is shown. For a simple inverse overcurrent (IOC) protection system it is necessary to determine how close two elements can be such that the upstream IOC element does not trip in response to a fault downstream of the downstream IOC element—a determination that is traditionally made using a time coordination interval (TCI) between the time current curves (TCC).

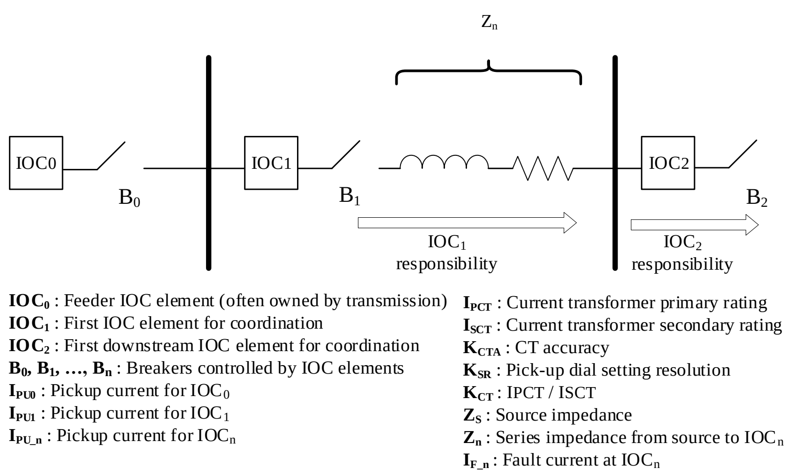

Figure 9. Simple protection coordination example using inverse overcurrent protection elements.

For coordination on a radial circuit with radial flow proper coordination is assured when:

$$I_{PU0} > I_{PU1} > I_{PUn} \tag{7}$$

The minimum detectable current ΔIMIN is the greater of

- KSR * KCT (Setting resolution * CT ratio)
- KCTA * IF_N (CT Accuracy * Fault Current)

- KCTA * IPCT (same as above with maximum current assumed).

The minimum impedance is therefore:

$$Z_{MIN} = \Delta I_{MIN} * \frac{Z_1^2}{(V_S - \Delta I_{MIN} * Z_1)} \tag{8}$$

For a fault current of 300 A and a CT accuracy of 5.0%, the minimum detectable current difference is 15 A. For a setting resolution of 0.1 and a CT ratio of 500/5 = 100, the minimum coordination current difference is 10 A. At 300 A fault current on a 7.62 kV system, Z_1 = 7,620/300 = 25.4Ω. Using the greater of 10 A and 15 A, the minimum impedance between IOC elements is $15*25.4^2$ / (7,620 – 15*25.4) = 1.33Ω

The protection design feeds into the proposed method by determining: (1) the investment options (protection devices, protection schemes), (2) the costs of the protection investments, and (3) the constraints of the potential protection investment locations.

For overcurrent protection, the distance constraint applies to the investment variable $w_{i,j}^S \in \{0,1\}$. The binary variable indicates whether a switch is built online (*i,j*). If $w_{1,2}^S = 1$ (adding a switch to line 1-2), then the adjacent line switch investment $w_{2,3}^S$ cannot be equal to 1 because it is too close to ensure proper coordination. The new constraint then becomes:

$$w_{1,2}^s + w_{2,3}^s \leq 1 \tag{9}$$

Based on the admittance matrix (*Y*), connectivity and impedances of the system are known. By processing the matrix, the constraints of sections that cannot have switches at the same time are determined. These constraints are only for coordinating overcurrent protection. Other investment options, such as relays with communication-assisted protection $\left(w_{i,j}^{cs}\right)$, will be added with different constraints including $c_{i,j}^{cs}$ (cost of investment $w_{i,j}^{cs}$) > $c_{i,j}^{s}$ (cost of investment $w_{i,j}^{S}$). The constraints are considered validated if an adequate protection scheme can be developed for design.

While the approach described in the previous sections for ensuring protection coordination is performed as a post-optimization verification, future work will examine integrating it into the optimization loops as shown in Figure 3.

4.0 Test System and Simulation Results

This section contains simulation and analysis results of the methods presented in Section III. Using a representative IEEE Distribution Test System, the methodology presented in Section III is demonstrated using the open-source OD&O tool [17]. The OD&O tool is used to determine the optimal set of upgrade options so that the two microgrids can support critical operations when the normal utility service is interrupted. The microgrids cannot support all of their coincidental peak critical loads when they operate individually. The goal of the optimization is to determine the least expensive combination of DERs and/or construction of tie lines that will enable the microgrids to support all of the critical end-use load when they are networked. For the simplicity of presenting the example batteries are not included as investment options. The optimization is conducted examining two fault/damage scenarios.

4.1 Test System

The test system used for this work is a modified version of the original IEEE 13 Node Test System [45]. Compared to the original system, the following changes have been made, as shown in Figure 10:

- addition of a transformer and switchgear at bus 671-1 to allow formation of microgrid 1 (MG#1) and MG#2
- addition of switchgear at node 632-1
- inclusion of 5,830 kVA of generation at node 684 and 2,580 kVA at node 692-1
- replacement of static loads with time-varying loads
- division of system loads into critical and non-critical loads to enable decisions about load shedding.

Figure 10 also shows the location of the tie line between the two microgrids that will be considered as an investment option. For the operation of the microgrids two assumptions are made. First, it is assumed that the two microgrids have been designed and deployed to support only a portion of the coincidental peak of their critical end-use loads when there is a loss of substation service. Therefore, they must shed a portion of their critical load when islanded independently. Second, the DERs are operated using traditional droop controls, such as those developed as part of the DOE Consortium for Electric Reliability Technology Solutions (CERTS) [46], [47].

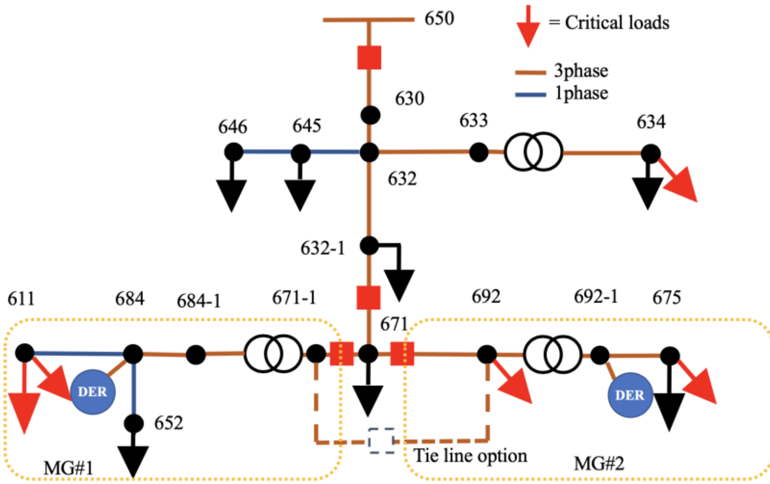

Figure 10. Modified IEEE 13 Node Test System

Next, it is assumed that the system operator wants to upgrade the microgrids so that all critical loads can be served when there is a loss of substation service. Given a range of damage scenarios, different investment options are evaluated to determine the most cost-effective solution.

4.1.1 Damage Scenario A

In the first damage scenario it is assumed that there is a three-phase to ground fault on the system between node 632 and 632-1, as shown in Figure 11. This is considered to be a "permanent" fault requiring 6-8 hours for the utility to locate and repair it. Both microgrids can support all of their critical loads at the start of the event, but they cannot do so for the duration of the event when operated individually. This is due to coincidental peak loads that prevent the microgrids from independently supplying all critical loads over the annual time horizon discussed in Section III. In this Damage Scenario, the primary distribution system is available for networked microgrid operations, but without investment the microgrids do not have this capability.

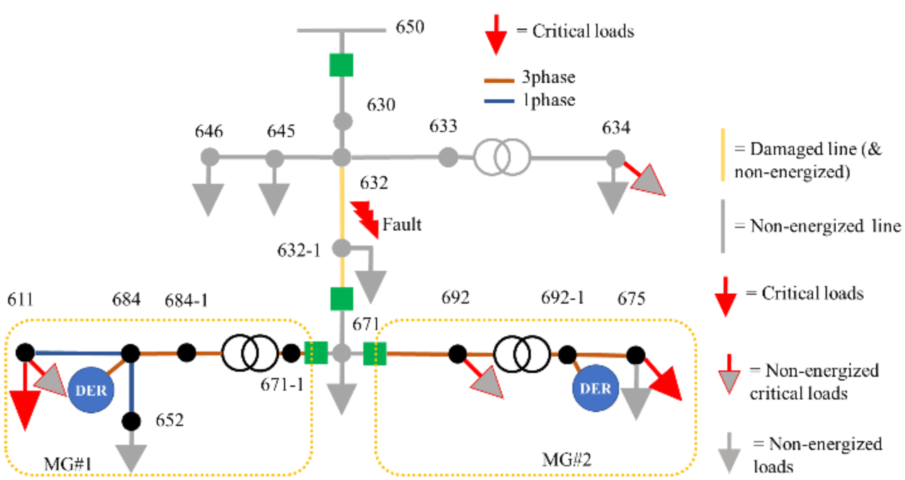

Figure 11. Configuration where microgrids operate independently under Damage Scenario A.

4.1.2 Damage Scenario B

In the second damage scenario, it is assumed that there is a three-phase to ground fault on the system between nodes 632-1 and 671, as shown in Figure 12. Similar to Damage Scenario A, both microgrids can support all of their critical loads at the start of the event but cannot do so for the duration of the event when operated individually. Unlike Damage Scenario A, the primary distribution system is not available for networked microgrid operations because of the location of the fault.

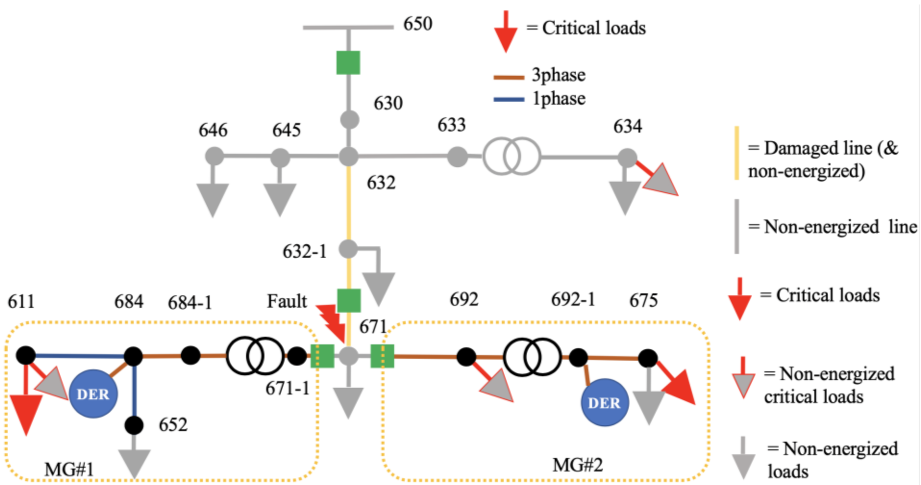

Figure 12. Configuration where microgrids operate independently under Damage Scenario B.

4.2 Resilience-layer Optimization

This section contains the optimization results from the OD&O tool, which evaluates the optimal combination of increasing DERs and/or the installation of the optional hardened tie line. The goal is to determine the most cost-effective combination of upgrades to ensure that all critical loads within MG#1 and MG#2 can be supplied during both damage scenarios.

4.2.1 Investment Case 1

The first investment case examines the installation of additional generation in each microgrid. In accordance with the process shown in Figure 3, increases in DER capacity are examined in the Outer-Layer optimization, and then the Resilience-Layer minimizes the load shedding required; specifically, ensuring non-critical loads are shed first, and critical loads as a last resort. In this investment case, only an increase of DERs is examined; the tie line is not considered an option.

In Investment Case 1, the optimization generates an output that requires the addition of 5,000 kVA of generation on node 684-1, and 2,500 kVA of additional generation on 692-1; because of the small size of the system, varying the locations of the DERs was not a variable, but the process supports variable locations. To be consistent with the CERTS-type controls assumed for the existing DERs, it will be assumed that the new DERs will also be interconnected with inverters. While inverter connect generation could be solar PV or batteries, this case will assume the added DERs are natural gas engines, which are interconnected through CERTS-type inverters [48]. These units are also selected because of their low emissions, which is a significant consideration for microgrids in urban and suburban environments.

The optimization ensures that all critical loads in the two microgrids can be supported over the required time frame if they are operated independently, because under Damage Scenario B, there is no possibility of networking the microgrids. Figure 13 shows the microgrids networked through the distribution system with the additional DER investments from Investment Case 1 under Damage Scenario A. This configuration is possible when there is sufficient generation capacity available within the microgrids to serve the load outside of the microgrids at node 671. Networking also provides increased reliability to the microgrids by sharing generation resources and the opportunity to operate more efficiently at lower load conditions [10].

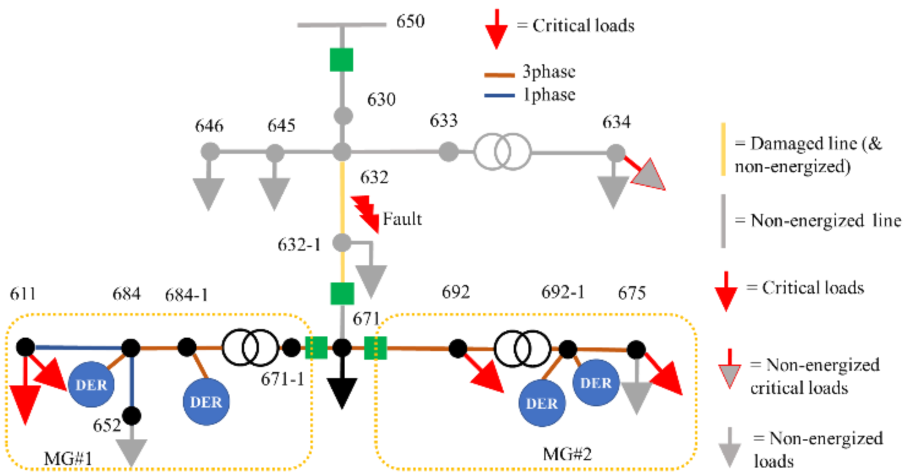

Figure 13. Configuration where microgrids are operating networked through the distribution system under Damage Scenario B.

4.2.2 Investment Case 2

Similar to the first investment case, the second case examines the addition of DERs, but it also examines the option of adding a new hardened tie line. Specifically, a tie lie that has a much lower probability of faults than the existing lines between the two microgrids. In this case, a dedicated tie line with physically reinforced support structures that are not adjacent to vegetation is considered.

In Investment Case 2, the optimization generates an output that requires the addition of 3,000 kVA of generation on node 684-1 and the addition of a hardened tie line between nodes 684-1 and 692. Because of the addition of the tie line, it is now possible to add DER at a single location, instead of in both microgrids. All critical loads in the two microgrids can be supported under both damage scenarios with lower DER investment than Investment Case 1 because networked operation is possible under both damage scenarios. Figure 14 shows the microgrids networked through the tie line with investments from Investment Case 2 under Damage Scenario B for which the distribution system is not available for networking. Under Damage Scenario A, the microgrids can network through the distribution system if sufficient generation is available to support the load at node 671.

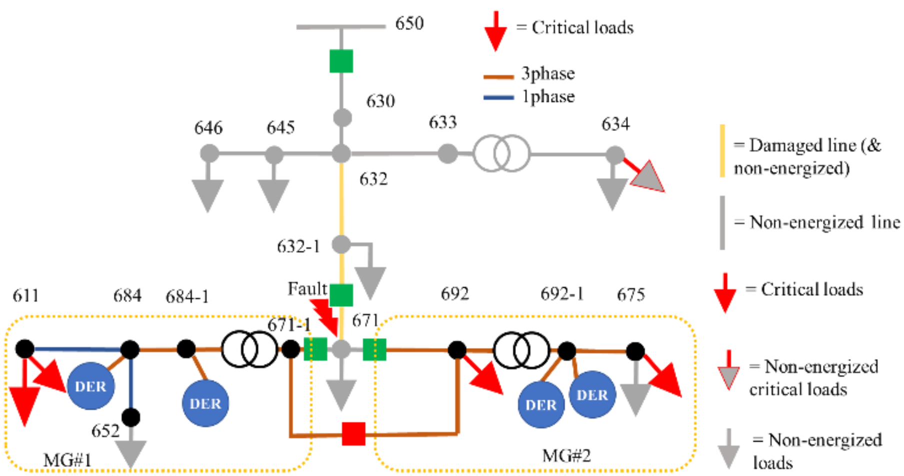

Figure 14. Configuration where microgrids are operating networked through the tie line under Damage Scenario B.

For Investment Case 2, the optimization yields a *12.6% reduction* in investment costs compared to Investment Case 1. As a result, it is considered to be the most cost-effective solution for the preliminary design.

If only damage scenario A is considered, the optimization yields lower DER investment similar to investment Case 2, and no tie line investment, because the distribution system is available for networking. This is the lowest cost solution, but it would not be able to support all the critical loads under a damage scenario similar to B, which makes networking through the distribution system impossible. This illustrates the importance of considering multiple different damage scenarios within the optimization.

4.3 Applicability of Constraints to Investment Case 2

With Investment Case 2 identified as the optimal solution, the next sections validate the associated stability and protection constraints.

4.3.1 Validation of Stability Constraints

It is necessary to validate the stability of both damage scenarios. The small-signal stability conditions are expressed in terms of the line parameters, load parameters, and inverter droop gains, as discussed in Section III. These stability conditions are sufficient closed-form distributed conditions with respect to a pair of buses, i.e., the closed-form expression of the stability boundary is a conservative estimate of the stability boundary computed using eigenvalue analysis. Numerical analysis is carried out to validate these small-signal stability estimates, consistent with the comparison in previously shown in Figure 7 and Figure 8. The plots of dynamic stability for *P-f* and *Q-V* droop gains, m_p and m_q respectively, are developed for the two microgrids in Damage Scenarios A and B of Investment Case 2, as shown in Figures 13 and 14, respectively.

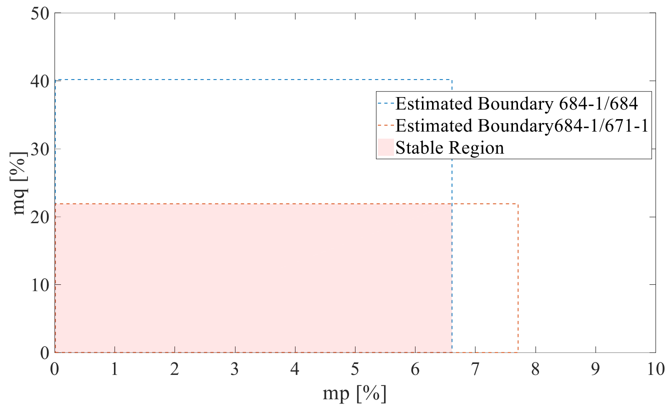

Figure 15. Small-signal stability results of Investment Case 1, Damage Scenario A.

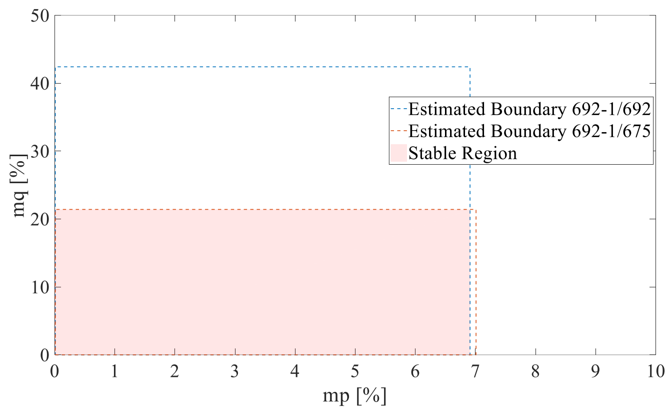

Figure 16. Small-signal stability results of Investment Case 1, Damage Scenario B.

The key observation from Figures 15 and 16 is that for Investment Case 2, the microgrid is small-signal stable if its m_p and m_q values are within the shaded regions. The stable regions in Figures 13 and 14 cover the range of typical droop values, and therefore small-signal stability can be achieved.

4.3.2 Validation of Protection Constraints

Because of the small size of the system depicted in Figure 10, it is relatively straightforward to determine whether the system can be protected using existing methods. For Investment Case 2, it was determined that traditional IOC protection can be implemented. Specifically, the impedance between line segments is large enough that proper IOC protection can be implemented. This is not to say that IOC protection is the best method, just that the preliminary design generated by the OD&O tool can be protected; specifically, the impedance of each of the lines in the system is greater than Z_{min} as calculated in (13).

5.0 Concluding Comments

The networking of deployed microgrids has the potential to increase the reliability, resiliency, and efficiency of supplying critical end-use loads. However, the complexity of considering the full range of networked microgrid operations can pose significant challenges when developing a preliminary design. This paper has presented an optimization process for the development of a preliminary design to network existing, i.e. brown field, microgrids.

To support the proposed method, a simple example case has been shown using an open-source tool developed by DOE. The simple example shows how a preliminary design can be developed by considering different investment options to support critical loads across multiple damage scenarios. The rapid development of an optimized preliminary design can reduce the time to deployment by providing a tractable foundation for the detailed design, and eventually for the final as-built design.

The work presented in this paper represents the first steps in an ongoing series of efforts being conducted at multiple DOE national laboratories. Future work is warranted to expand the scope of optimization options, examine an increased range of networked microgrids operations, and to examine the impact of various statutory and regulatory decisions.

6.0 References

[1] "IEEE Guide for Electric Power Distribution Reliability Indicies," *IEEE Std.". 1366-2012*, pp. 1-43, 2012.

[2] "Economic Benefits of Increasing Electric Grid Resilience to Weather Outages," Executive Office of the President, Washington D.C., August 2013.

[3] "Economic Impact of Hurricane Sandy Potential Economic Activity Lost and Gained in New Jersey and Mew York," U. S. Department of Commerce, Economics and Statistics Administration, Office of the Chief Economist, September 2013.

[4] A. Wood and B. Wollenberg, "Power Generation, Operation, and Control, Second Edition," John Wiley & Sons, Inc., 1996.

[5] "Microgrid Effects and Opportunities for Utilities," Burns & McDonnel, Kansas City, MO, 2013.

[6] K. Hirose, T. Shimakage, and H. Irie, "The Sendai Microgrid Operational Experience in the Aftermath of the Tohuku Earthquake: A Case Studt," NNT Faciliaites Inc., Case Study, 2013.

[7] J. Stamp and J. Stinebaugh, "SPIDERS Project: Fort Carson Preliminary Design Summary," Sandia National Laboratories, Albuquerque, NM, SAND2012-4324, March 2012.

[8] M. Shahidehpour and J. Clair, "A Functional Microgrid for Enhancing Resiliency," *Electricity Journal*, vol. 25, no. 8, October 2012, pp. 21-28.

[9] K. P. Schneider, F. K. Tuffner, M. A. Elizondo, C. C. Liu, Y. Xu, and D. Ton, "Evaluating the Feasibility to use Micrograms as a Resiliency Resource," *IEEE Trans. on Smart Grid*, vol. 8, no. 2, pp. 687-696, March 2017.

[10] S. N. Backhaus, L. Dobriansky, S. Glover, C.C. Liu, P. Looney, S. Mashayekh, A. Pratt, K. P. Schneider, M.Stadler, M. Starke, J. Wang, and M. Yue, "Networked Microgrids Scoping Study," LA-UR-16-27399, Los Alamos National Laboratory, Los Alamos, New Mexico, 2016.

[11] Z. Li, M. Shahidehpour, F. Aminifar, A. Alabdulwahad, and Y. Al-Turki, "Networked Microgrids for Enhancing the Power System Resilience," *Proceedings of the IEEE*, vol. 105, no. 7, pp. 1289-1310, July 2017.

[12] Z. Wang, B. Chen, J. Wang, and J. Kim, "Decentralized Energy Management System for Networked Microgrids in Grid-Connected and Islanded Modes," *IEEE Trans. on Smart Grid*, vol. 7, no. 2, pp. 1097-1105, March 2016.

[13] Y. Li, P. Zhang, and P. Luh, "Formal Analysis of Networked Microgrid Dynamics," *IEEE Trans. on Power Systems*," vol. 33, no. 3, pp. 3418-3427, May 2018.

[14] K. P. Schneider, N. Radhakrishnan, Y. Tang, F. K. Tuffner, C. C. Liu, J. Xie, and D. Ton, "Improving Primary Frequency Response to Support Networked Microgrid Operations," *IEEE Trans. on Power Systems*, vol. 34, no. 1, pp. 659-667, Jan. 2019.

[15] M. Johnson, "JCTD Overview Technical Overview Phases 1-3," Fall Federal Utility Partnership Working Group (FUPWG) Seminar, 2015. Accessed: April 1, 2020. [Online]. Available: https://www.energy.gov/sites/prod/files/2015/11/f27/fupwg_fall2015_johnson.pdf

[16] M. Shahidehpour, Z. Li, S. Bahramirad, Z. Li, and W. Tran, "Networked Microgrids: Exploring the Possibilities of the IIT-Bronzeville Grid," *IEEE Power and Energy Magazine*, vol. 15, no. 4, pp. 63-71, July 2017.

[17] Operations & Design Optimization for Networked Microgrids Accessed: April 1, 2020. [Online]. Available: https://github.com/lanl-ansi/ODO

[18] F. Flores-Espino, J. Giraldez, and A. Pratt, "Networked Microgrid Optimal Design and Operations Tool: Regulatory and Business Environment Study," NREL/TP-5D00-70944, 2020.

[19] P. Kundur, *Power System Stability and Control*, McGraw-Hill, New York, NY, 1994.

[20] M. Farrokhabadi et al., "Microgrid Stability Definitions, Analysis, and Examples," *IEEE Trans. on Power Systems*, vol. 35, no. 1, pp. 13-29, Jan. 2020.

[21] "IEEE Standard for Interconnecting Distributed Resources with Electric Power Systems," *IEEE Std 1547a-2014*. pp. 1–16, 2015.

[22] Kröger, O., Coffrin, C., Hijazi, H. and Nagarajan, H., 2018, June. Juniper: an open-source nonlinear branch-and-bound solver in Julia. In International Conference on the Integration of Constraint Programming, Artificial Intelligence, and Operations Research (pp. 377-386). Springer, Cham.

[23] A. Barnes, H. Nagarajan, E. Yamangil, R. Bent, "Resilient Design of Large-Scale Distribution Feeders with Networked Microgrids", Electric Power Systems Research, 2019.

[24] S. K. K. Hari, K. Sundar, H. Nagarajan, R. Bent, S. Backhaus, "Hierarchical Control Predictive Algorithms for Optimal Design and Operation of Microgrids", in proc. Power Systems Computation Conference, 2018.

[25] G. Byeon, P. Van Hentenryck, R. Bent, H. Nagarajan, "Communication-Constrained Expansion Planning for Resilient Distribution Systems", Informs Journal on Computing, 2019

[26] S.C. Madathil, E. Yamangil, H. Nagarajan, A. Barnes, R. Bent, S. Backhaus, S.J. Mason, S. Mashayekh, M. Stadler, "Resilient Off-grid Microgrids: Capacity Planning and N-1 Security", 2017, *IEEE Trans. on Smart Grid*, vol. 9, no. 6, pp. 6511-6521, Nov. 2018.
[27] Nagarajan, H., Yamangil, E., Bent, R., Van Hentenryck, P. and Backhaus, S., 2016, June. Optimal resilient transmission grid design. In 2016 Power Systems Computation Conference (PSCC) (pp. 1-7). IEEE.
[28] P. Kundur, J. Paserba, V. Ajjarapu, G. Andersson, A. Bose, C. Canizares, N. Hatziargyriou, D. hill, A. Stankovic, C. Taylor, T. Van Custem, and V. Vittal, "Definition and Classification of Power System Stability," *IEEE Trans. on Power Systems*, vol. 19, no. 2 pp. 1398-1401, May 2004.
[29] K. P. Schneider, F. K. Tuffner, M. A. Elizondo, J. Hansen, J. C. Fuller and D. P. Chassin, "Adaptive Dynamic Simulations for Distribution Systems Using Multistate Load Models," in *IEEE Trans. on Smart Grid*, vol. 10, no. 2, pp. 2257-2266, March 2019.
[30] S. Ihara and F. C. Schweppe, "Physically Based Modeling of Cold Load Pickup," in *IEEE Trans. on Power Apparatus and Systems*, vol. PAS-100, no. 9, pp. 4142-4150, Sept. 1981.
[31] R. Majumder, "Some Aspects of Stability in Microgrids," in *IEEE Trans. on Power Systems*, vol. 28, no. 3, pp. 3243-3252, Aug. 2013.
[32] W. Du, Q. Jiang, M. J. Erickson and R. H. Lasseter, "Voltage-Source Control of PV Inverter in a CERTS Microgrid," in *IEEE Trans. on Power Delivery*, vol. 29, no. 4, pp. 1726-1734, Aug. 2014.
[33] N. Pogaku, M. Prodanovic and T. C. Green, "Modeling, Analysis and Testing of Autonomous Operation of an Inverter-Based Microgrid," in *IEEE Trans. on Power Electronics*, vol. 22, no. 2, pp. 613-625, March 2007.
[34] P. A. Mendoza-Araya and G. Venkataramanan, "Impedance matching based stability criteria for AC microgrids," *in proc.* IEEE Energy Conversion Congress and Exposition (ECCE), Pittsburgh, PA, 2014, pp. 1558-1565.
[35] S. V. Iyer, M. N. Belur and M. C. Chandorkar, "A Generalized Computational Method to Determine Stability of a Multi-inverter Microgrid," in *IEEE Trans. on Power Electronics*, vol. 25, no. 9, pp. 2420-2432, Sept. 2010.
[36] P. Vorobev, P. Huang, M. A. Hosani, J. L. Kirtley and K. Turitsyn, "A framework for development of universal rules for microgrids stability and control," in proc. IEEE 56th Annual Conference on Decision and Control (CDC), Melbourne, VIC, 2017, pp. 5125-5130.
[37] P. Vorobev, P. Huang, M. Al Hosani, J. L. Kirtley and K. Turitsyn, "High-Fidelity Model Order Reduction for Microgrids Stability Assessment," in *IEEE Trans. on Power Systems*, vol. 33, no. 1, pp. 874-887, Jan. 2018.
[38] X. Guo, Z. Lu, B. Wang, X. Sun, L. Wang and J. M. Guerrero, "Dynamic Phasors-Based Modeling and Stability Analysis of Droop-Controlled Inverters for Microgrid Applications," in *IEEE Trans. on Smart Grid,* vol. 5, no. 6, pp. 2980-2987, Nov. 2014.
[39] J.-J. E. Slotine and W. Li, "Applied Nonlinear Control," Englewood Cliffs, NJ: Prentice Hall, 1991.
[40] J. L. Blackburn, "Protective Relaying Principles and Applications, Third Edition," CRC Press, 2006.
[41] N. S. Gurule, J. Hernandez-Alvidrez, M. J. Reno, A. Summers, S. Gonzalez, and J. Flicker, "Grid-forming Inverter Experimental Testing of Fault Current Contributions," *in proc.* IEEE Photovoltaic Specialists Conference, 2019.
[42] S. S. Venkata, M. J. Reno, W. Bower, S. Manson, J. Reilly, and G. W. Sey Jr, "Microgrid Protection: Advancing the State of the Art," Sandia National Laboratories, SAND2019-3167, 2019.
[43] S. Hossain-McKenzie, E. C. Piesciorovsky, M. J. Reno, and J. C. Hambrick, "Microgrid Fault Location: Challenges and Solutions," Sandia National Laboratories, SAND2018-6745, 2018.
[44] B. Reimer, T. Khalili, A. Bidram, M. J. Reno, and R. C. Mathews, "Optimal Protection Relay Placement in Microgrids," *in proc.* IEEE Kansas Power and Energy Conference, 2020.
[45] K. P. Schneider, B. A. Mather, B. C. Pal, C. W. Ten, G. J. Shirek, H. Zhu, J. C. Fuller, J. L. R. Pereira, L. F. Ochoa, L. R. de Araujo, R. C. Dugan, S. Matthias, S. Paudyal, T. E. McDermott, and W. Kersting, "Analytic Considerations and Design Basis for the IEEE Distribution Test Feeders," *IEEE Trans. on Power Systems*, vol. 33, no. 3, pp. 3181-3188, May 2018.
[46] R. H. Lasseter, J. H. Eto, B. Schenkman, J. Stevens, H. Vollkommer, D. Klapp, E. Linton, and J. Roy, "CERTS Microgrid Laboratory Test Bed," *IEEE Trans. on Power Delivery*, vol. 26, no. 1, pp. 325-332, Jan. 2011.
[47] R. Panora, J. E. Gehret, M. M. Furse, and R. H. Lasseter, "Real-World Performance of a CERTS Microgrid in Manhattan," *IEEE Trans. on Sustainable Energy*, vol. 5, no. 4, pp. 1356-1360, Oct. 2014.
[48] Tecogen Advanced Modular CHP System. Accessed: April 1, 2020. [Online]. Available: https://www.tecogen.com/chp-cogeneration/inverde
[49] S. P. Nandanoori, S. Kundu, W. Du, F. Tuffner, and K. P. Schneider. "Distributed Small-signal Stability Conditions for Inverter-based Unbalanced Microgrids," *Accepted IEEE Trans. on Power Systems*, Mar. 2020.

Pacific Northwest National Laboratory

902 Battelle Boulevard
P.O. Box 999
Richland, WA 99354
1-888-375-PNNL (7665)

www.pnnl.gov